

Fully Integrated Si-Rich Silicon Nitride Wavelength Converter Based on Bragg Scattering Intermodal Four-Wave Mixing

Valerio Vitali^(1,2,*), Thalía Domínguez Bucio⁽¹⁾, Hao Liu⁽¹⁾, José Manuel Luque González⁽³⁾, Francisco Jurado-Romero⁽³⁾, Alejandro Ortega-Moñux⁽³⁾, Glenn Churchill⁽¹⁾, James C. Gates⁽¹⁾, James Hillier⁽⁴⁾, Nikolaos Kalfagiannis⁽⁴⁾, Daniele Melati⁽⁵⁾, Jens H. Schmid⁽⁶⁾, Ilaria Cristiani⁽²⁾, Pavel Cheben⁽⁶⁾, J. Gonzalo Wangüemert-Pérez⁽³⁾, Íñigo Molina-Fernández⁽³⁾, Frederic Gardes⁽¹⁾, Cosimo Lacava⁽²⁾, Periklis Petropoulos⁽¹⁾

⁽¹⁾ Optoelectronics Research Centre, University of Southampton, Southampton, SO17 1BJ, UK,

⁽²⁾ Electrical, Computer and Biomedical Engineering Department, University of Pavia, Pavia, 27100, Italy, *valerio.vitali@unipv.it

⁽³⁾ Telecommunication Research Institute (TELMA), Universidad de Málaga, CEI Andalucía TECH, E.T.S.I. Telecomunicación, 29010 Málaga, Spain,

⁽⁴⁾ School of Science and Technology, Nottingham Trent University, Nottingham, NG11 8NS, UK,

⁽⁵⁾ Centre de Nanosciences et de Nanotechnologies, Université Paris-Saclay, CNRS, 91120 Palaiseau, France,

⁽⁶⁾ Advanced Electronics and Photonics Research Center, National Research Council Canada, 1200 Montreal Road, Ottawa, ON K1A 0R6, Canada.

Abstract *We report the demonstration of an integrated silicon-rich silicon nitride wavelength converter based on Bragg scattering intermodal four-wave mixing process. The system integrates mode conversion, multiplexing and de-multiplexing functionalities on chip. Broadband signal conversion with a 3dB bandwidth exceeding 70 nm is demonstrated. ©2023 The Author(s)*

Introduction

Modern optical transmission systems need to respond to an insatiable demand for ever-more bandwidth to transmit the continuously increasing amount of data across the world. One possible approach to tackle this challenge is based on the use of new frequency windows of the electromagnetic spectrum that have not been heavily used up to now. One option might be the utilization of the L and U bands (1565 - 1675 nm). In these new systems, the ability to generate and manipulate wavelengths is an enabling feature. Third-order nonlinearity-based devices offer the possibility to generate new wavelengths through parametric processes such as those based on four-wave mixing (FWM)^[1]. Recently, integrated devices based on intermodal FWM (IM-FWM) processes, where nonlinear effects take place between different spatial modes, have been investigated, and have shown a considerable potential to respond to the needs of novel transmission systems^{[2]-[5]}. Indeed, dispersion-engineered multimode nonlinear waveguides offer an extra degree of freedom in the design by using multiple spatial modes to fulfill the required phase matching. This allows for broadband operation in multiple discrete spectral bands, even at locations far away from the pump wavelength(s). IM-FWM pro-

cesses in integrated silicon or silicon-rich (Si-rich) silicon nitride waveguides have been reported in the past years, employing either continuous wave (CW)^{[2],[6]} or pulsed optical pump sources^{[3],[7]}. Among these demonstrations, some of them used Bragg scattering (BS) IM-FWM to generate clean idler signals (free from the pump noise) in the C or L bands^{[2],[6]}. These first attempts showed the potential of these schemes, however, their experimental configurations were complex and suffered from the lack of integrated components aimed at processing and controlling the spatial shapes of the involved waves, eventually introducing extra losses in the whole system. This, in turn, limited the efficiency of the IM-FWM, even when relatively high pump power levels were used.

In this paper, we discuss the experimental characterization of a fully integrated wavelength converter based on a Si-rich silicon nitride platform. The device integrates the whole set of functionalities needed to perform wavelength conversion in the intermodal regime, starting from three (two pumps and one signal) seeding waves coupled from single-mode optical fibres (SMF-28). This eliminates the need for external and bulky mode conversion components, strongly reduces the overall loss of the full device, and eliminates the need to filter the pumps out at the output of

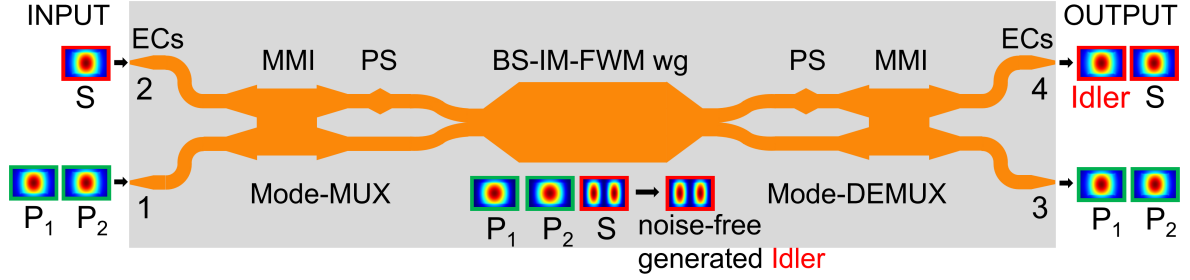


Fig. 1: Schematic layout of the fully integrated wavelength converter and BS-IM-FWM working principle. ECs: edge couplers; MMI: multimode interference coupler; PS: phase shifter; wg: waveguide; P_1 : Pump 1, P_2 : Pump 2; S : Signal.

the device. The integrated system is capable of generating idler components covering the whole U-band starting from an L-band signal, with a 3dB bandwidth (BW) exceeding 70 nm by using optical pumps placed in the C- and L-band.

Operation principle and device configuration

The device was designed to perform wavelength conversion using the BS-IM-FWM process in a multimode waveguide. An efficient (phase-matched) BS-IM-FWM process is achieved when the propagation constants of the interacting waves satisfy the momentum conservation (as well as the energy conservation). For small pump-to-pump wavelength detunings, this occurs when the derivative of the propagation constant, i.e. the inverse group velocity (IGV), in one mode is the same as that in another mode. If the IGV curves of the two modes under consideration are parallel across a large frequency range, the phase matching condition can be maintained even when the two pumps are largely detuned from one another^[2]. In our configuration, two pumps were placed in the waveguide fundamental TE (TE_{00}) mode while a seeding noise-free signal was placed in the first-order TE (TE_{10}) mode, allowing the generation of a noise-free idler in the TE_{10} mode. The device was designed and fabricated using our in-house Si-rich silicon nitride platform. Details regarding the fabrication process can be found in^{[8],[9]}. The platform is composed of a 300 nm thick layer of Si-rich silicon nitride (refractive index $n = 2.41$ measured at 1550 nm) grown on a 3 μm thick layer of thermal silicon dioxide. Our numerical results showed that BS-IM-FWM can be achieved with no efficiency decrease from the C to the U band, using the first two TE modes of a multimode waveguide with 6.10 μm width and 300 nm thickness. A schematic layout of the device is shown in Fig. 1. Inverted taper-based edge couplers (ECs) were designed to couple signals incoming from

SMF-28 fibres. Two pump waves were coupled at port 1, while the seed signal was coupled at port 2. The combination of a multimode interference (MMI) coupler, followed by a 90-degree phase shifter (PS) placed in one of the two MMI output arms and a sinusoidal-profile Y-branch was used as a mode converter and multiplexer (MUX) (overall footprint of 4 $\mu\text{m} \times 121 \mu\text{m}$), so that the signal was converted in the TE_{10} mode, while the pumps remained in the TE_{00} mode (more details on the working principle can be found in^[10]). The three waves were then coupled into the multimode waveguide section (length $L = 1.07$ cm). A specular section was realized at the output, allowing to convert all the TE_{10} modes to TE_{00} modes and de-multiplex them. Finally, two inverted taper-based ECs were used to couple the waves to the required output SMF-28 fibres. It is worth noting that the idler and seeding signal can be both extracted from port 4, while the residual pumps are sent to port 3, thus automatically eliminating the need to filter the pumps out from the signals.

Experimental setup and results

The experimental setup is shown in Fig. 2.

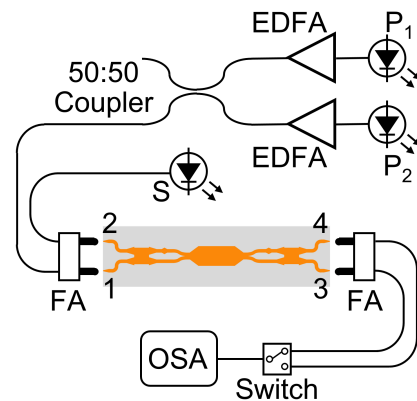


Fig. 2: Simplified sketch of the experimental setup used in the nonlinear experiments. EDFA: Erbium doped fibre amplifier; FA: fibre array; OSA: optical spectrum analyzer.

The optical pumps (P_1 , P_2) were generated using two polarization-maintaining (PM) tunable

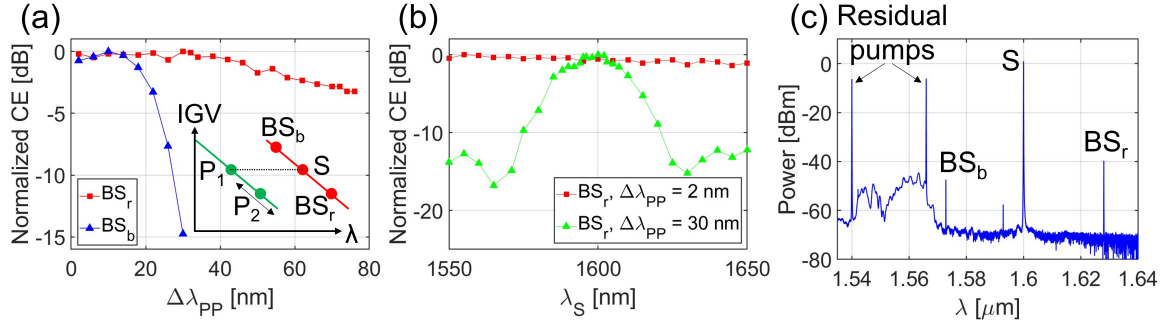


Fig. 3: (a) Normalized CE for BS_b (blue triangles) and BS_r (red squares) idlers as a function of $\Delta\lambda_{PP}$ with $\lambda_{P1} = 1540$ nm and $\lambda_S = 1600$ nm; the inset shows the pumps-signal configuration used in this experiment, with a fixed λ_{P1} and λ_S and a varying λ_{P2} ; (b) Normalized CE for BS_r idler as a function of λ_S for $\Delta\lambda_{PP} = 2$ nm (red squares) and $\Delta\lambda_{PP} = 30$ nm (green triangles), with $\lambda_{P1} = 1540$ nm; (c) example of a spectrum acquired from port 4 for $\lambda_{P1} = 1540$ nm, $\lambda_{P2} = 1566$ nm and $\lambda_S = 1600$ nm.

lasers followed by two PM Erbium-doped fibre amplifiers (EDFAs). The pumps were coupled together with a 50:50 PM coupler and sent to port 1 of the device. Similarly, the seeding signal (S) was generated using a third PM source and sent to port 2 of the device. At the output, the signal and idler on port 4 and the residual pumps on port 3 were collected and sent via an optical switch to an optical spectrum analyzer (OSA). One input and one output fibre array (FA) with two lensed PM fibres each were used to couple light in and out of the chip. The linear behavior of the device was initially characterized. A total fibre-to-fibre loss of around 5 dB was measured between ports 1 to 3 and ports 2 to 4, while a loss of around 20 dB was estimated when crossing input-output ports were considered (ports 1 to 4 and ports 2 to 3). Two different sets of nonlinear measurements were then carried out using a total launched power in the waveguide equal to 27.6 dBm. In the first measurement campaign, the first pump (P_1) was placed at 1540 nm, while the second one (P_2) was varied from 1542 to 1616 nm aiming at characterizing the pump-to-pump detuning BW ($\Delta\lambda_{PP} = P_2 - P_1$) of the BS-IM-FWM process. According to the design simulation, the signal wavelength λ_S was set to 1600 nm to ensure phase matching with P_1 (see the inset of Fig. 3 (a)). Fig. 3 (a) shows the normalized conversion efficiency (CE) measured for the blue- and red-shifted idlers (BS_b and BS_r , respectively). Results show a small decrease in CE for the BS_r idler, while a much narrower BW, as expected from the theory^[2], is observed for the BS_b idler. A 3dB $\Delta\lambda_{PP}$ BW of 72 nm was measured for BS_r , corresponding to an idler generated from 1602 to 1678 nm, as expected from the energy conservation. In the second set of measurements, the signal-detuning BW was evaluated: the two

pumps were placed at $\lambda_{P1} = 1540$ nm and $\lambda_{P2} = 1542$ nm, while the position of λ_S was varied between 1550 and 1650 nm. Using this wavelength configuration, the BS-IM-FWM CE values were recorded for the BS_r idler. The results are reported in Fig. 3 (b) and show no CE reduction, even for signal detuning values of ± 50 nm (relative to $\lambda_S = 1600$ nm). The measurements were then repeated with $\Delta\lambda_{PP} = 30$ nm ($\lambda_{P1} = 1540$ nm, $\lambda_{P2} = 1570$ nm). The normalized CE is reported in Fig. 3 (b). In this case, the phase matching condition for BS_r was not retained across the full range of scanned wavelengths, and a 3dB BW of 25 nm was observed, centered at around $\lambda_S = 1600$ nm. An example of a recorded spectrum measured at port 4 for $\Delta\lambda_{PP} = 26$ nm is reported in Fig. 3 (c). The maximum CE was measured to be equal to -41 dB, mainly limited by the short length of the nonlinear waveguide in our particular implementation and the material losses.

Conclusions

In this paper, we presented the realization of an integrated, BS-IM-FWM-based wavelength converter realized on a Si-rich silicon nitride platform. Mode conversion, multiplexing and demultiplexing were performed on-chip by using a broadband MMI and PS in cascade. Our device showed wavelength conversion with a 3dB BW exceeding 70 nm, which represents, to the best of our knowledge, the widest BW ever reported for a multi-mode FWM-based system. We believe that the proposed device represents a significant step towards the realization of a fully-integrated, highly-tunable frequency synthesizer able to operate in optical bands hundreds of nanometers apart.

Acknowledgements

This research was funded by the UK's EPSRC through grant EP/T007303/1 and EP/R003076/1.

References

- [1] J. Leuthold, C. Koos, and W. Freude, "Nonlinear silicon photonics", *Nature photonics*, vol. 4, no. 8, pp. 535–544, 2010. DOI: 10.1038/nphoton.2010.185.
- [2] C. Lacava, T. D. Bucio, A. Khokhar, *et al.*, "Intermodal frequency generation in silicon-rich silicon nitride waveguides", *Photonics Research*, vol. 7, no. 6, pp. 615–621, 2019. DOI: 10.1364/PRJ.7.000615.
- [3] S. Signorini, M. Mancinelli, M. Borghi, *et al.*, "Intermodal four-wave mixing in silicon waveguides", *Photonics Research*, vol. 6, no. 8, pp. 805–814, 2018. DOI: 10.1364/PRJ.6.000805.
- [4] Z. Xu, Q. Jin, Z. Tu, and S. Gao, "All-optical wavelength conversion for telecommunication mode-division multiplexing signals in integrated silicon waveguides", *Applied Optics*, vol. 57, no. 18, pp. 5036–5042, 2018. DOI: 10.1364/AO.57.005036.
- [5] T. Kernetzky, G. Ronniger, U. Höfler, L. Zimmermann, and N. Hanik, "Numerical optimization and cw measurements of soi waveguides for ultra-broadband c-to-o-band conversion", in *2021 European Conference on Optical Communication (ECOC)*, IEEE, 2021, pp. 1–4. DOI: 10.1109/ECOC52684.2021.9605944.
- [6] C. Lacava, M. A. Ettabib, T. D. Bucio, *et al.*, "Intermodal bragg-scattering four wave mixing in silicon waveguides", *Journal of Lightwave Technology*, vol. 37, no. 7, pp. 1680–1685, 2019. DOI: 10.1109/JLT.2019.2901401.
- [7] S. Signorini, M. Finazzer, M. Bernard, M. Ghulinyan, G. Pucker, and L. Pavesi, "Silicon photonics chip for intermodal four wave mixing on a broad wavelength range", *Frontiers in Physics*, p. 128, 2019. DOI: 10.3389/fphy.2019.00128.
- [8] C. Lacava, S. Stankovic, A. Z. Khokhar, *et al.*, "Si-rich silicon nitride for nonlinear signal processing applications", *Scientific reports*, vol. 7, no. 1, pp. 1–13, 2017. DOI: 10.1038/s41598-017-00062-6.
- [9] F. Gardes, A. Shooa, G. De Paoli, *et al.*, "A review of capabilities and scope for hybrid integration offered by silicon-nitride-based photonic integrated circuits", *Sensors*, vol. 22, no. 11, p. 4227, 2022. DOI: 10.3390/s22114227.
- [10] D. González-Andrade, A. Dias, J. G. Wangüemert-Pérez, *et al.*, "Experimental demonstration of a broadband mode converter and multiplexer based on sub-wavelength grating waveguides", *Optics & Laser Technology*, vol. 129, p. 106297, 2020. DOI: 10.1016/j.optlastec.2020.106297.